Highly efficient solar hydrogen production through the use of bifacial photovoltaics and membrane electrolysis

S.M.S. Privitera [a,*], M. Muller [b], W. Zwaygardt [b], M. Carmo [b], R.G. Milazzo [a], P. Zani [c], M. Leonardi [a], F. Maita [a,d], A. Canino [c], M. Foti [c], F. Bizzarri [e], C. Gerardi [c], S.A. Lombardo [a]

[a] Consiglio Nazionale Delle Ricerche (CNR) - Istituto per La Microelettronica e Microsistemi (IMM), Zona Industriale, Ottava Strada 5, 95121, Catania, Italy
[b] Institute of Energy and Climate Research, Electrochemical Process Engineering (IEK-14), Forschungszentrum Jülich GmbH, Wilhelm-Johnen-Str., 52428, Jülich, Germany
[c] Enel Green Power, Zona Industriale, Contrada Blocco Torrazze, 95121, Catania, Italy
[d] Consiglio Nazionale Delle Ricerche (CNR) - Istituto per La Microelettronica e Microsistemi (IMM), Rome Unit, Via del Fosso Cavaliere 100, 00133 Rome, Italy
[e] Enel Green Power, Viale Regina Margherita, 125, 00198, Rome, Italy

HIGHLIGHTS

- Monofacial Silicon Heterojunction module produces 3.7 gr of H_2 $h^{-1}m^{-2}$ at 1 sun.
- Monofacial Silicon Heterojunction gives 11.5% of solar to hydrogen (STH) efficiency.
- Bifacial operation increases the production up to 4.2 gr of H_2 $h^{-1}m^{-2}$ at 1 sun.
- 13.5% STH average increase in bifacial mode, compared to monofacial.
- System stable upon outdoor operation up to 55 h.

GRAPHICAL ABSTRACT
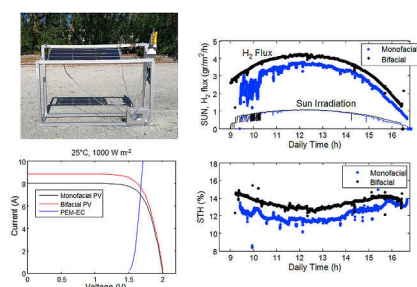
ABSTRACT

The large-scale implementation of solar hydrogen production requires an optimal combination of photovoltaic systems with suitably-designed electrochemical cells, possibly avoiding power electronics for DC-DC conversion, to decrease costs. Here, a stable, solar-driven water splitting system is presented, obtained through the direct connection of a state-of-the-art proton exchange membrane (PEM) electrolyzer to a bifacial silicon heterojunction (SHJ) solar module of three cells in series with total area of 730 cm^2. The bifaciality of the solar module has been optimized through modeling in terms of the number of cells, module height and inclination. During outdoor operation in the standard monofacial configuration, the system is able to produce 3.7 gr of H_2 $h^{-1}m^{-2}$ with an irradiation of 1000 W m^{-2} and a solar-to-hydrogen efficiency (STH) of 11.55%. The same system operating in bifacial mode gives rise to a higher H_2 flux and STH efficiency, reaching values of 4.2 gr of H_2 $h^{-1}m^{-2}$ and STH of 13.5%. Such a noticeable difference is achieved through the collection of albedo radiation from the ground by the bifacial PV system. The system has been tested outdoors for more than 55 h, exhibiting very good endurance, with no appreciable change in production and efficiency.

* Corresponding author.
  E-mail addresses: stefania.privitera@imm.cnr.it, stefaniams.privitera@gmail.com (S.M.S. Privitera).

1. Introduction

Mitigating climate change urgently requires the adoption of renewable energy, CO_2 sequestration and carbon-neutral energy technologies. Amongst these, photovoltaics (PV) are becoming one of the most important. PV energy prices are now highly competitive compared to conventional fossil fuel sources, but one major issue remains, namely the intrinsic randomness of solar power due to the day/night cycle, geographical location, climate and seasonal variations, etc. The solution to this is the storage of solar energy at economically-viable costs. A very promising approach is that of solar fuels, i.e., the production of carbon-neutral fuels using solar energy, such as H_2 by means of water electrolysis. For this purpose, one possible solution is a photovoltaic system with suitably-designed electrochemical cells, possibly avoiding power electronics for DC-DC conversion to decrease costs and increase system reliability. This concept, initially proposed in the 1970s [1], has recently gained new interest, as it can now be boosted by the major advancements in electrochemical cell and photovoltaic module technologies that have taken place in the intervening decades. However, to be practical for large-scale deployment, the cost of solar hydrogen generation must still be significantly reduced.

Some figures of merit that can be used to estimate H_2 generation costs are solar-to-hydrogen efficiency (STH) and H_2 flow per unit area of a PV cell. Very recently, a record STH efficiency [2] of 30% was reported through the use of a concentrated triple junction solar cell made of InGaP, GaAs and GaInNAs and a polymer electrolyte membrane electrolyser cell (PEM-EC) with Pt and Ir catalysts operating at 80 °C. Using this system, with a solar concentration of 42 SUN, the authors were able to convert 70% of produced electrical energy into hydrogen. Other remarkable results with comparable approaches have also been obtained by other research groups [3–5]. However, the cost of a concentrated, multi-junction solar system is still fairly high by comparison to silicon PV solar cells and additional costs, such as heating of the PEM-EC (up to 80 °C) on one hand, as well as the cooling of the concentrated system, must also be taken into account. To reduce H_2 production costs, one approach is to use silicon-based solar modules. c-Si modules have been implemented in solar-hydrogen devices, yielding an STH efficiency of 9.7% [6,7]. More recently, Silicon Heterojunction (SHJ) solar cells [8] have been connected to an alkaline electrolysis system with Ni foam electrodes operating under basic electrolytes (1 M KOH), as well as to a PEM-EC system containing Pt and IrO_x catalyst coatings on a 177 μm-thick Nafion membrane. With both systems, by illuminating a PV area of 5.7 cm^2, under a solar simulator at 1000 W m^{-2}, an STH efficiency of 14.2% has been demonstrated.

On the other hand, in the last few years the Si PV research community has paid ever more attention to the development of bifacial Si PV modules. With this technology, a PV module collects sunlight from both the front side, as with conventional PV, and from the back side, by collecting the albedo radiation diffused by the ground. With proper installation and system design, such an approach produces a noticeable increase in the PV energy yield. For this reason, the problem of the optimization of the bifacial module installation is widely investigated in the literature and in the PV community, as it holds great promise for the further improvement of PV technology [9–16].

In this study it is shown that, compared to the reference monofacial conventional system, a well-designed system consisting of a bifacial Si heterojunction (SHJ) photovoltaic mini-module, directly coupled to a PEM electrolyzer, provides a noticeable boost in H_2 production efficiency. The system optimization is also discussed and an optimal design is defined. The experimental demonstration of such a system, shows a noticeable improvement in efficiency thanks to its bifaciality. Another investigated aspect is the system scalability. Thus far, demonstrations in the literature have been performed using laboratory-scale devices. In this paper, we take a realistic approach, using commercially-manufactured SHJ solar cells of 15.6 × 15.6 cm^2 in size, and connected in series and laminated in a mini module of three cells, with a

total area of 730 cm^2, to provide sufficient voltage to enable water splitting. A fully operational system has been studied under a large range of outdoor illumination conditions, with negligible ohmic losses and no observable system degradation.

2. Experimental

2.1. Photovoltaic system design

For the solar cells, bifacial Si HJT cells, based on the amorphous Si/crystalline Si heterojunction, developed by Enel Green Power at its 3SUN facility, have been employed. As these have an open circuit voltage at 1 SUN above 730 mV, a mini-module of three such cells is sufficient to power the PEM electrolysis cell used for water splitting and H_2 generation, which requires voltages well above 1.5 V. Mini-modules of three cells placed in series by copper ribbons and laminated in a transparent, EVA-backed polyethylene double substrate, were adopted. The PV cells are bifacial, with a very high bifaciality factor, equal to about 90%.

2.2. The PEM-EC design

The PEM-EC system is composed of different functional layers that ensure a good media supply to the electrochemically-active layers, a relatively high power density and high efficiency. An overview of the setup is given in Fig. 1 and the components are listed in Table 1.

The two endplates are necessary for pressing all the components and ensuring low contact resistance. The cell itself consists of flow field structures made of expanded carbon material, which is machined by means of water jet cutting. The diffusion layer is in contact with the flow structure and has a porosity of 80% and electrical conductivity. The electrochemically active layer is made of a mixture of Nafion and Iridium, with a catalyst loading of 2.7 mg cm^{-2} Ir at the anode. At the cathode, platinum is the catalyst material and catalyst loading is 0.7 mg cm^{-2}_{Pt}. The electrochemically active layers are in contact with a Nafion HP membrane with a thickness of 20 μm. The electrodes area is 10 cm^2.

2.3. Experimental setup

The PV mini-module is directly coupled to the PEM-EC cell through the use of low-resistance copper cables. The current flowing through the system is evaluated with the voltage drop across a 1.30 mΩ resistor in series. Meanwhile, the horizontal solar radiation is evaluated using an MS-40 EKO piranometer, while the solar radiation at the PV module tilt angle orientation is measured by a calibrated Si reference PV cell. All the data are acquired through a CR1000 Campbell Scientific data logger. Fig. 2(a) and (b) display a schematic drawing and picture of the system, respectively.

The PEM-EC is operated at ambient pressure and low temperature of less than 40 °C. Under these conditions, previous measurements have shown that the cell has a Faradaic efficiency of about 100% [17], so in the present experiments, the H_2 flux is evaluated by the instantaneous
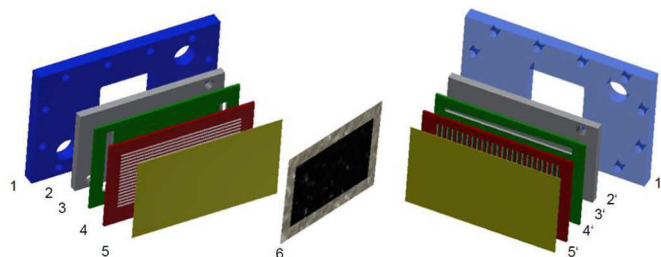

Fig. 1. Schematic of the electrolysis cell design, which is coupled to the PV panel (anode side left, cathode side right).

Table 1
PEM-EC system components.

Anode	Component	Cathode
1	End plate	1′
2	Power supply plate	2′
3	External flow distribution	3′
4	Internal flow structure	4′
5	Conductive diffusion layer	5′
6	Catalytic coated membrane	6

electrical current flowing in the system, assuming a 100% Faradaic efficiency. The water is stored in an atmospheric open tank with volume of 300 ml. The water is supplied to the EC device through 6 mm PTFE tubes. Hydrogen and Oxygen in this experiment are not stored, but are released in the atmosphere. There is no water circulation pump, since it is not necessary.

3. Results and discussion

3.1. Optimal bifacial conditions determination

Bifaciality requires optimization in order to take full advantage of the ground albedo radiation. For this purpose, a model has been recently developed, to predict bifacial solar module installation optimization, based on the numerical evaluation of the photocurrent collected by the back side of the bifacial solar cell [18,19]. The model is in three dimensions (3D) and more complex compared to mathematically-simpler 2D models. It is based on the evaluation of the solid angle under which each ground element sees the solar cells by assuming that under a 2π steradian solid angle, it isotropically diffuses the horizontal solar radiation incident on the element reduced by the ground albedo factor α. α is assumed to be equal to normal incidence reflectivity. In fact, the ground 'colour' has been also taken into account by considering the wavelength (λ) dependence of α and the λ dependence of the external quantum efficiency (EQE) of the solar cell. Then, numerical integration across the entire solar spectrum and all of the ground area is performed, the series connection of all cells is evaluated and the maximum power point (MPP) of the PV system is calculated. The model has been validated through a comparison with experimental data taken on a four-cell PV mini-module by best fitting the data of an MPP power as a function of solar irradiation, module height, module inclination with respect to the horizontal plane and ground albedo [18]. Such a model has also been applied to evaluate the weight of the perimeter zones surrounding a PV installation (not possible with a 2D model) and to quantitatively estimate the energy yield advantage of bifaciality and of the use of uniaxial solar trackers [19].

The model has been applied in this context to evaluate the best possible bifacial PV system design to drive a water-splitting PEM-EC cell. For the sun irradiation as a function of solar time, the spring equinox day has been considered, since it provides the average throughout the year of the daily solar irradiation and of the daylight duration. The latitude and

longitude of Catania - Passo Martino (37°24′N, 15°1′E), where the experiments have been performed, has been considered.

Fig. 3 (a) and (b) reports the daily energy yield of a three-cell bifacial PV system with an average ground albedo of 30%, like the one we used. The cells are in series, facing to the south and all in line along the east-west (local parallel) direction. Two parameters are changed in Fig. 3: (a) the inclination (tilt angle) of the module with respect to the horizontal plane at a constant module height of 50 cm; (b) the module height at a constant tilt of 35°. In Fig. 3(a), a clear maximum is evident at approximately 35–40°, close to the local latitude. This is in good agreement with the evaluations of [20] for monofacial PV systems. From Fig. 3(b), it is evident that at a height above 40 cm, the energy yield increase drops. A further evaluation is the best possible PV module configuration to be coupled to the PEM-EC cell. As it is required to have three PV cell in series to achieve sufficient voltage for water-splitting, the number of cells in the PV module should be a multiple of 3, i.e., 3, 6, 9, 12, 15, etc., organized either as one row in the east-west direction of 3, 6, 12, 15 cells, etc., or as two rows (e.g., two rows of three or six cells, etc.), or as three rows (e.g., three rows of two, three, or five cells, etc.). In fact, as the number of cells in the PV module increases, the dispersion of illumination on the cell's back-side increases, which worsens the overall PV module's energy yield. In fact, all the cells are in series and the overall MPP is dominated by the cell with the worst back-side illumination. Therefore, to reduce such back-side illumination dispersion, it is convenient to reduce the PV module's size. Through our model, it is found that the best configurations in terms of PV energy yield per unit area are those made by one row with three cells, or two rows with three cells. Therefore, based on the results of Fig. 3 (a) and (b) and of the above considerations, the PV system has been designed by using three cells organized in one row, with a 35° tilt angle and a 50 cm module height.

Further optimization can be obtained by considering the ground albedo. Fig. 3(c) reports the daily energy yield of the horizontal three-cell PV system with a 35° tilt angle and 50 cm height as a function of the average ground albedo. The zero albedo corresponds to the monofacial energy yield. The PV energy yield increases with the albedo. In our experiment, the average albedo is 30%, so the expected PV energy yield increase, compared to the monofacial system, is +13.6%. Moreover, as the albedo increases, the expected energy yield increase (YAF) is about +6 Whr per m^2 and per % albedo, equal to +0.45% per % albedo.

3.2. Effect of bifaciality on hydrogen production

Fig. 4 shows the current-voltage (I–V (a)) and power-voltage (P–V (b)) characteristics of the system components, that is the PV minimodule, and the PEM-EC cell, acquired in standard conditions (25 °C and 1000 W m^{-2} incident solar radiation). Bifacial and monofacial characteristics are shown as red and back solid lines, respectively. The monofacial module is exactly the same bifacial PV module, but with an added white sheet placed on the module's back side to shield the back-side illumination from the ground albedo. The PV module efficiency is
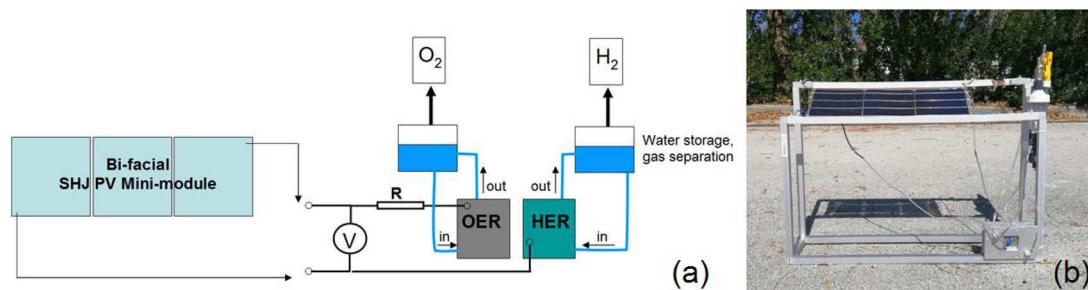

Fig. 2. (a) Schematic of the coupled PV-PEM-EC system, showing as dark lines the electrical connections and as blue lines the liquid/gas pipes; (b) picture of the system. (For interpretation of the references to colour in this figure legend, the reader is referred to the Web version of this article.)
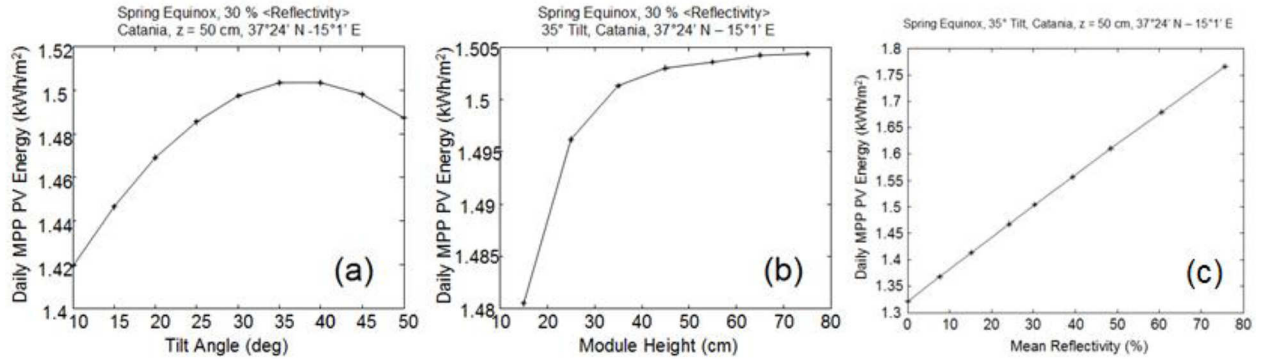
Fig. 3. (a) Daily energy yield with an average ground albedo of 30% as a function of module inclination (tilt angle), constant height of 50 cm; (b) Daily energy yield with an average ground albedo of 30% as a function of module height at a fixed tilt angle of 35°; (c) Daily energy yield of a three-cell PV module with a 35° tilt angle and 50 cm height as a function of the average ground reflectivity.

defined as the ratio between the module maximum electrical power P_{mpp}, shown in Fig. 4(b) and the incident solar optical power (corresponding to an optical power density P_{in}). For $P_{in} = 1000$ W m^{-2} the obtained efficiency value η_{PV} for the PV mini-module operating in monofacial mode is 16.4%, calculated as:

$$\eta_{PV} = \frac{P_{mpp}}{NAP_{in}} \tag{1}$$

where N is the number of cells in the mini-module (equal to 3) and A is the cell area (243.36 cm^2).

The bifacial module shows a +12% increase of power in the MPP, and therefore of the effective efficiency, compared to the monofacial module, which is in good agreement with the simulations shown in Fig. 3 (ground with about 30% average albedo). The characteristics of the PEM electrolyzer at 25 °C are shown in Fig. 4 (a) and (b) as blue lines.

In general, the operating point of the EC-PV system, defined by the couple (V_c, I_c), is obtained as the intersection of the EC cell and PV module I–V curves, as visible in Fig. 4(a). Then, the STH efficiency is defined as:

$$STH = 1.23\, I_c\, \eta_F / (NAP_{in}) \tag{2}$$

Assuming a 100% faradaic efficiency η_F, for a given PV module with short circuit current I_{SC}, the maximum achievable STH is:

$$STH_{max} = 1.23\, I_{SC} / (NAP_{in}) \tag{3}$$

In particular, from data shown in Fig. 4(a) and (b), the STH_{max} is equal to 13.7% in monofacial mode. For the EC cell the I–V curve can be approximated to a linear relationship, that is:

$$V_c = V_{TH} + R_{EC}\, I_c \tag{4}$$

where V_{TH} is the threshold voltage above which the EC current is larger than zero, and R_{EC} is the EC cell series resistance. From Eqs. (2)–(4) I_c, V_c, and STH can be then evaluated. Fig. 4 (c) and (d) show the calculated V_c values and the ratio between the STH and STH_{max}, respectively, as a function of V_{TH} and R_{EC}. As expected, as V_{TH} and R_{EC} decrease, V_c
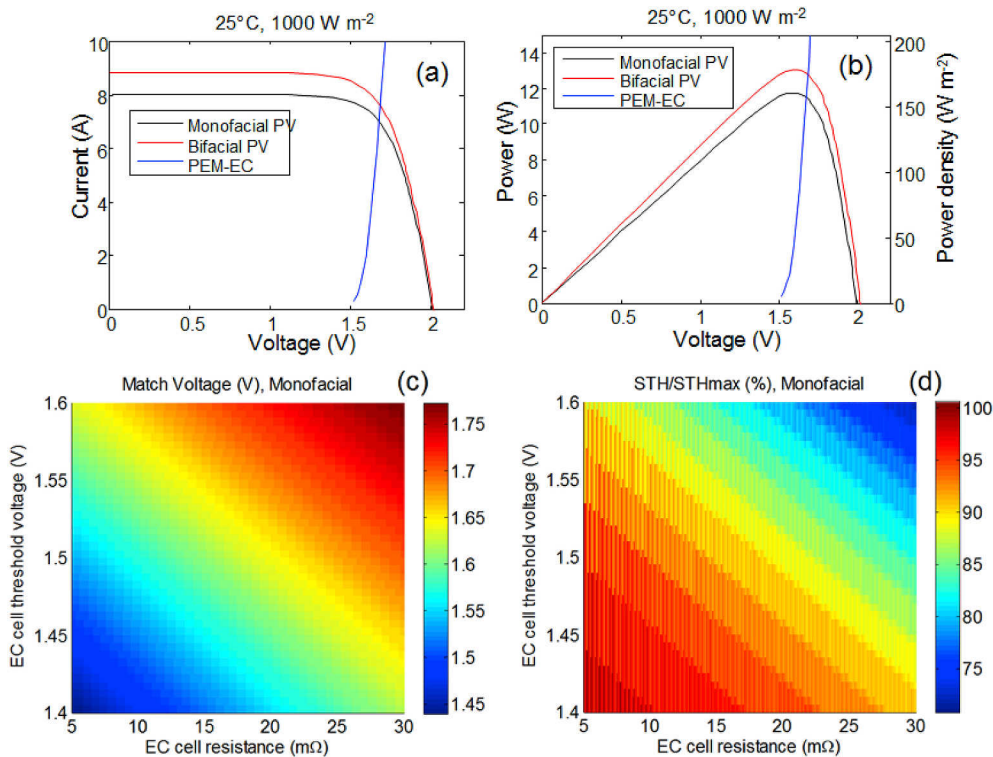

Fig. 4. (a) Current-voltage characteristics of the three-cell PV module in monofacial and bifacial operation and of the PEM electrolyzer; (b) power-voltage characteristics of the three-cell PV module in monofacial and bifacial operation and of the PEM electrolyzer. The right axis shows the corresponding PV module power density. (c) Calculated matching voltage V_c as a function of the EC cell resistance R_{EC} and of the EC threshold voltage V_{TH}; (d) Ratio between the calculated STH value at V_c and the maximum STH, STH_{max}, as a function of the EC cell resistance R_{EC} and of the EC threshold voltage V_{TH}.
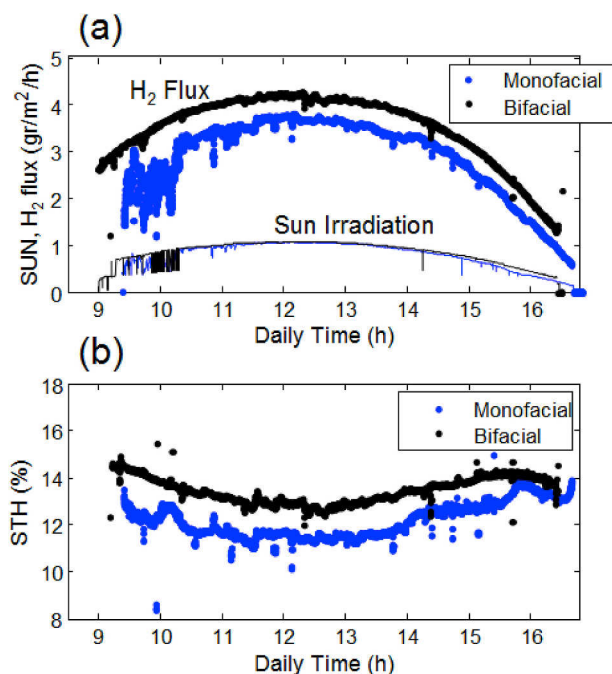
Fig. 5. (a) Solar irradiation conditions (SUN) and H$_2$ flux per unit PV area, measured during outdoor operation in a bifacial or monofacial configuration. The same system was tested on two different days, exhibiting similar solar irradiation and weather conditions; (b) comparison of the STH efficiency.

decreases and the STH increases. In the present experiment V$_{TH}$ = 1.55 V and R$_{EC}$ = 13 mΩ, therefore V$_c$ is approximately at the PV module maximum power point, i.e. V$_c$ = V$_{mpp}$ = 1.65 V. From Fig. 4 (d) the expected STH is about 90% of STH$_{max}$, therefore the system is designed to achieve a good matching.

Fig. 5 presents the comparison of H$_2$ flux (a) and STH (b) of the same system operating in bifacial and monofacial mode, measured outdoor from approximately 9 a.m. to 4 p.m. The data were measured on two different days with the same system (except for the use of the white sheet on the PV module's back side in the case of monofacial operation). The solar irradiation conditions (reported in Fig. 5(a)) were measured through the calibrated Si reference cell, while the PV and EC module temperature (not reported) on the two days were very similar. It is evident that during bifacial operation, the H$_2$ flux and STH efficiency were larger, with an average increase, with respect to the STH efficiency obtained with the monofacial system, of 14.7% and 12.2% between 11 a.m. and 2 p.m., respectively. Such a noticeable difference is attributed to the effective collection of albedo radiation from the ground by the bifacial PV system. Note that such a H$_2$ flux production increase is achieved with no extra equipment, such as the mirrors of Fresnel lenses for solar radiation concentration, etc. Instead, only the optimal use of ground albedo is exploited.

Fig. 6 reports the comparison of the bifacial PV-EC system operating simply with the ground albedo due to only the asphalt (See Fig. 2(b)), or with an increased albedo due to the addition of a 1 m^2 plastic white panel placed on the ground below the PV module.

Fig. 7(a) shows the reflectivity as a function of wavelength measured for the asphalt and for the white panel. The experimental setup is shown in Fig. 7(b). As the average albedo with the white panel is 53%, against the value of 30% of the asphalt, according to the simulation in Fig. 3(c), the yield increase should be the YAF times the albedo increase, equal to +20%, which is a total of 0.45 × 20 = 9% expected yield increase. As shown by the data in Fig. 6, the increased albedo obtained with the white panel on the ground produces an increase of H$_2$ flux and an STH efficiency of about +5.5%, with respect to the bifacial panel results. The experimentally-derived value is lower then expected from the
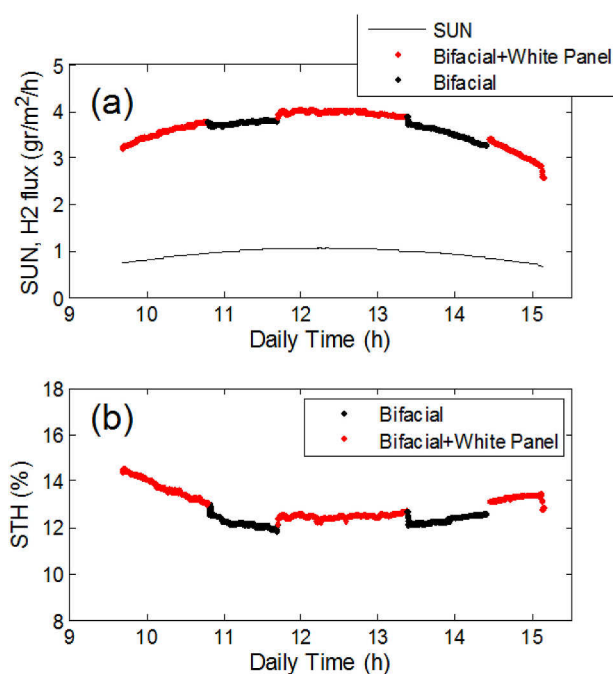
simulation, but this is reasonable, as the albedo increase is only partial, given the limited dimension of the white sheet (1 m^2) used for the experiments. Nevertheless, the results indicate that higher ground albedo can effectively increase the hydrogen production yield.

3.3. Long term stability

Fig. 8 shows the experimental results taken on the system on eight different days. H$_2$ flux, STH Efficiency and solar irradiation data, together with the average daily temperature are reported in the figure. As it is clearly evident, weather, temperature and solar irradiation conditions varied across a wide range of values, as it can be seen from an inspection of the data of Fig. 8. Nevertheless, no appreciable change of STH efficiency was observed for a total operation time of about 55 h, indicating that the proposed approach is promising in terms of performance and endurance.
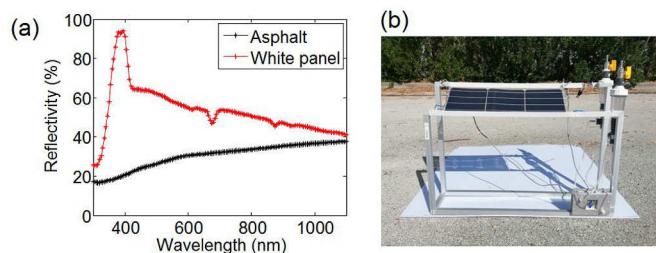

Fig. 6. Solar irradiation conditions (SUN) and H$_2$ flux per unit PV area, measured during outdoor operation in a bifacial configuration operating with the ground albedo due to the asphalt (black symbols) or with an increased albedo due to the addition of a 1 m^2 plastic white panel placed on the ground below the PV module (red symbols); (b) STH efficiency as a function of daily time. (For interpretation of the references to colour in this figure legend, the reader is referred to the Web version of this article.)

Fig. 7. (a) Reflectivity versus wavelength of the asphalt and of the white plastic panel; (b) picture of the experimental setup, using the 1 m^2 white plastic panel on the ground.
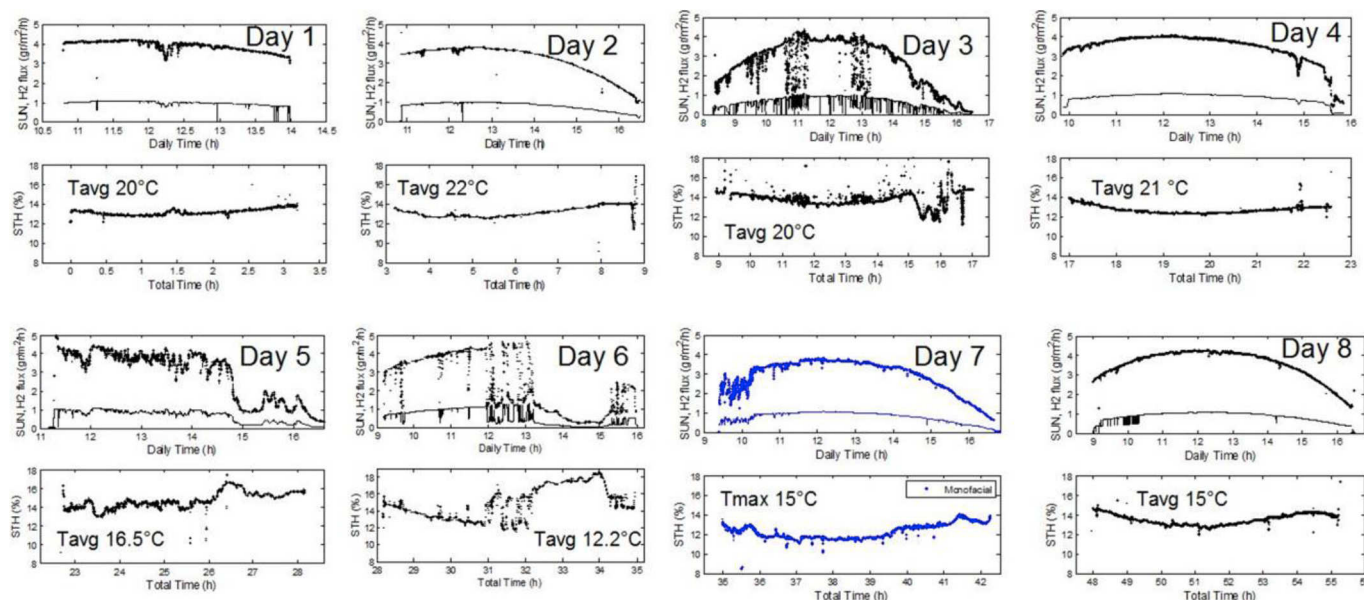
Fig. 8. Solar irradiation conditions (SUN), H_2 flux per unit PV area and STH efficiency measured during outdoor operation for eight days, with a total operation of more than 55 h, without efficiency degradation.

4. Conclusions

In summary, the optimization of bifaciality has been studied for a coupled bifacial SHJ PV module – PEM-EC system, for solar H_2 production. Optimization was performed by numerical modeling. Then, an experimental demonstration of the optimized system was developed and tested. Experimental data show, in good agreement with modeling, that bifaciality, with a 30% average ground albedo, and with no additional equipment, such as lenses, mirrors, etc., provides a boost of STH Efficiency and solar H_2 flux of +13%, with respect to the STH efficiency obtained with the monofacial system. The improvement of the produced hydrogen flux can be further increased up to about +22% for a 50% average albedo.

The results can be considered a promising starting point for further development of a larger system in which long term operation and stability will be tested.

Declaration of competing interest

The authors declare that they have no known competing financial interests or personal relationships that could have appeared to influence the work reported in this paper.

CRediT authorship contribution statement

S.M.S. Privitera: Conceptualization, Methodology, Data curation, Writing - original draft. **M. Muller:** Methodology, Data curation, Conceptualization, Writing - review & editing. **W. Zwaygardt:** Methodology, Data curation, Conceptualization, Writing - review & editing. **M. Carmo:** Conceptualization, Writing - review & editing. **R.G. Milazzo:** Data curation. **P. Zani:** Data curation, Methodology. **M. Leonardi:** Data curation. **F. Maita:** Data curation. **A. Canino:** Resources. **M. Foti:** Resources. **F. Bizzarri:** Resources. **C. Gerardi:** Resources. **S.A. Lombardo:** Data curation, Methodology, Conceptualization, Writing - original draft, Funding acquisition.

Acknowledgement

This work was funded through the PECSYS Project. The project received funding from the Fuel Cells and Hydrogen 2 Joint Undertaking

References

[1] A. Fujishima, K. Honda, Electrochemical photolysis of water at a semiconductor electrode, Nature 283 (1972) 37.

[2] Jieyang Jia, Linsey C. Seitz, Jesse D. Benck, Yijie Huo, Yusi Chen, Jia Wei Desmond Ng, Taner Bilir, James S. Harris, Thomas F. Jaramillo, Solar water splitting by photovoltaic-electrolysis with a solar-to-hydrogen efficiency over 30%, Nat. Commun. 7 (2016) 13237, https://doi.org/10.1038/ncomms13237.

[3] G. Peharz, et al., Solar hydrogen production by water splitting with a conversion efficiency of 18%, Int. J. Hydrogen Energy 32 (2007) 3248–3252, https://doi.org/10.1016/j.ijhydene.2017.07.069.

[4] A. Fallish, et al., Hydrogen concentrator demonstrator module with 19.8% solar-to-hydrogen conversion efficiency according to the higher heating value, Int. J. Hydrogen Energy 42 (2017) 26804–26815, https://doi.org/10.1016/j.ijhydene.2017.07.069.

[5] A. Nakamura, Y. Ota, K. Koike, Y. Hidaka, K. Nishioka, M. Sugiyama, K. Fujii, A 24.4% solar to hydrogen energy conversion efficiency by combining concentrator photovoltaic modules and electrochemical cells, Appl. Phys. Expr. 8 (2015) 107101, 2015.

[6] J.W. Ager, M. Shaner, K. Walczak, I.D. Sharp, S. Ardo, Experimental demonstrations of spontaneous, solar-driven photoelectrochemical water splitting, Energy Environ. Sci. 8 (2015) 2811.

[7] R. Cox, J.Z. Lee, D.G. Nocera, T. Buonassisi, Ten-percent solar-to-fuel conversion with nonprecious materials, Proc. Natl. Acad. Sci. U.S.A. 111 (2014) 14057, https://doi.org/10.1073/pnas.1414290111.

[8] J.-W. Schuttauf, M.A. Modestino, E. Chinello, D. Lambelet, A. Delfino, D. Dominé, A. Faes, M. Despeisse, J. Bailat, D. Psaltis, C. Moser, C. Ballif, Solar-to-Hydrogen production at 14.2% efficiency with silicon photovoltaics and earth-abundant electrocatalysts, J. Electrochem. Soc. 163 (2016) F1177–F1181.

[9] U.A. Yusufoglu, T.H. Lee, T. Pletzer, A. Halm, L. Koduvelikulathu, C. Comparotto, R. Kopecek, H. Kurz, Simulation of energy production by bifacial modules with revision of ground reflection, Energy Procedia 55 (2014) 389, https://doi.org/10.1016/j.egypro.2014.08.111.

[10] U.A. Yusufoglu, T.M. Pletzer, L.J. Koduvelikulathu, C. Comparotto, R. Kopecek, H. Kurz, Analysis of the annual performance of bifacial modules and optimization methods, IEEE J. Photovolt. 5 (2015) 320–328, https://doi.org/10.1109/JPHOTOV.2014.2364406.

[11] I. Shoukry, J. Libal, R. Kopecek, E. Wefringhaus, J. Werner, Modelling of bifacial gain for stand-alone and in-field installed bifacial PV modules, Energy Procedia 92 (2016) 600–608, https://doi.org/10.1016/j.egypro.2016.07.025.

[12] J. Appelbaum, Bifacial photovoltaic panels field, Renew. Energy 85 (2016) 338–343, https://doi.org/10.1016/j.renene.2015.06.050.

[13] C.W. Hansen, D.M. Riley, C. Deline, F. Toor, J.S. Stein, A detailed performance model for bifacial PV modules, in: Proceedings of the 33rd European Photovoltaic Solar Energy Conference and Exhibition, Amsterdam, The Netherlands, 25–29 September 2017, https://doi.org/10.4229/EUPVSEC20172017-6BV.2.35.

[14] C. Deline, S. MacAlpine, B. Marion, F. Toor, A. Asgharzadeh, J.S. Stein, Assessment of bifacial photovoltaic module power rating methodologies—inside and out, IEEE J. Photovolt. 7 (2017) 575–580, https://doi.org/10.1109/JPHOTOV.2017.2650565.

[15] X. Sun, M.R. Khan, C. Deline, M.A. Alam, Optimization and performance of bifacial solar modules: a global perspective, Appl. Energy 212 (2018) 1601–1610, https://doi.org/10.1016/j.apenergy.2017.12.041.

[16] D. Chudinzow, J. Haas, G. Díaz-Ferrán, S. Moreno-Leiva, L. Eltrop, Simulating the energy yield of a bifacial photovoltaic power plant, Sol. Energy 183 (2019) 812–822, https://doi.org/10.1016/j.solener.2019.03.071.

[17] G. Tjarks, A. Gibelhaus, F. Lanzerath, M. Müller, A. Bardow, D. Stolten, Energetically-optimal PEM electrolyzer pressure in power-to-gas plants, Appl. Energy 218 (2018) 192–198, https://doi.org/10.1016/j.apenergy.2018.02.155.

[18] F. Ricco Galluzzo, A. Canino, C. Gerardi, S.A. Lombardo, A new model for predicting bifacial PV modules performance: first validation results, in: Proceedings of the 46th IEEE Photovoltaic Specialists Conference (PVSC 46), Chicago, IL, USA, 16–21 June 2019.

[19] F. Ricco Galluzzo, P.E. Zani, M. Foti, A. Canino, C. Gerardi, S. Lombardo, Numerical modeling of bifacial PV string performance: perimeter effect and influence of uniaxial solar trackers, Energies 13 (2020) 869, https://doi.org/10.3390/en13040869.

[20] D. Jain, M. Lalwani, A review on optimal inclination angles for solar arrays, Int. J. Renew. Energy Resour. 7 (2017) 1053–1061.